applied sciences

MDPI

Article

Experimental Analysis and Verification of the Influence on the Elastic Recovery Coefficient of Wheat

Jizhong Wang, Weipeng Zhang, Fengzhu Wang, Yangchun Liu, Bo Zhao and Xianfa Fang *

National Key Laboratory of Agricultural Equipment Technology, China Academy of Agricultural Mechanization Science Group Co., Ltd., Beijing 100083, China
* Correspondence: fangboshi2023@163.com

Abstract: To establish a collision model of wheat grains impacting a force plate with a piezoelectric sensor, and to investigate the influence of the elastic recovery coefficient on the sensor's detection accuracy during the collision process, this study employed object kinematic principles to construct a wheat elastic recovery coefficient measurement device. This device ascertains the elastic properties of wheat during collisions and determines the elastic recovery coefficient of the wheat collision model. The wheat variety Jinan No. 17 was selected for testing, and the effects of the contact material, grain drop height, material thickness, and grain moisture content on the collision recovery coefficient during the collision process were analyzed through single-factor and multi-factor experiments. The experimental results demonstrate that the collision recovery coefficient of wheat grains increases with the stiffness of the collision materials for different materials. The grain recovery coefficient of wheat exhibits a downward trend with increasing falling height and moisture content, while it tends to rise as the material thickness increases. Data analysis and comparison reveal that, given the determination of the collision material, the moisture content of wheat exerts the most significant effect on the elastic recovery coefficient, followed by material thickness, while the influence of falling height is less pronounced. The findings of this study can provide data support for simulation testing and product design of wheat combine harvester cleaning screen body mechanisms and wheat seeders.

Keywords: response surface method; collision model; elastic recovery coefficient; elastic characteristics; kinematics

check for updates

Citation: Wang, J.; Zhang, W.; Wang, F.; Liu, Y.; Zhao, B.; Fang, X. Experimental Analysis and Verification of the Influence on the Elastic Recovery Coefficient of Wheat. *Appl. Sci.* **2023**, *13*, 5481. https://doi.org/10.3390/app13095481

Academic Editors: Li Pei, Jia Shi, Hua Bai, Yunhui Mei and Pingjuan Niu

Received: 12 March 2023
Revised: 31 March 2023
Accepted: 4 April 2023
Published: 28 April 2023

Copyright: © 2023 by the authors. Licensee MDPI, Basel, Switzerland. This article is an open access article distributed under the terms and conditions of the Creative Commons Attribution (CC BY) license (https://creativecommons.org/licenses/by/4.0/).

1. Introduction

The elastic characteristics of wheat constitute fundamental data for designing cleaning shakers and sowing plates in wheat harvesters. During the screening operation of the harvester cleaning system, wheat undergoes collisions and ejections, either with other wheat particles or with the screen body, within the screening bin. The efficacy of the cleaning system's screen selection is influenced by these collision and ejection motions. Furthermore, an array of collision and ejection movements occurs as wheat is transported within the seed harvester, seed scraper, and seed feeder during seeding operations. Consequently, studying the elastic characteristics of wheat bears considerable significance for enhancing the vibratory screening mechanisms of wheat cleaning and the functional components of wheat seeders.

The recovery coefficient represents the capacity of an object to recover from deformation during collisions, first introduced by Newton as he employed the instantaneous impulse method to resolve the collision issue of rigid body systems. This coefficient serves as an essential parameter for characterizing alterations in the motion state of objects pre- and post-collision. Currently, extensive research has been conducted on elastic collision theory, the exploration recovery coefficient, and the methodologies for measuring these coefficients both domestically and internationally. Ning et al. assessed the elastic recovery coefficient for two soybean varieties [1]. Liu et al. analyzed and calibrated the elastic recovery coefficient for wheat seeds via a wheat accumulation test, subsequently deriving

the discrete element parameters of wheat [2]. Li et al. measured maize seeds' recovery coefficient and established the contact parameters between maize seeds and seeders [3]. Kong investigated and analyzed the recovery coefficient for seed cotton; Yang et al. measured and analyzed the collision recovery coefficient for castor capsules [4]. Liu determined the collision recovery coefficient for oil sunflower grains [5]. Wen gauged the recovery coefficient of garlic seeds [6]. Zhang measured the recovery coefficient of mung beans [7].

In this study, Ji'nan 17 wheat seed was selected, and based on the analysis of the principle of kinematics, a wheat seed falling impact test platform was designed. The effects of the contact material, grain fall height, material thickness, and grain water content on the collision recovery coefficient of wheat were investigated through single-factor and multi-factor experiments, providing a basic data reference for the design optimization of harvesting and seeding machinery structure and the simulation modeling of loss sensor [8,9].

2. Materials and Methods

2.1. Test Materials

Four wheat samples with varying moisture content (10%, 13%, 15%, and 18%) were prepared by screening complete and plump wheat grains to simulate harvest conditions [10]. The working components of the combine harvester during wheat harvesting are typically composed of rubber, structural steel, and other materials. In order to simulate the collision recovery coefficient in the realistic environment of wheat grain collision, the test materials selected were structural steel Q235 and rubber. The material properties of the chosen materials can be ascertained by consulting the material library parameters as displayed in Table 1 [11].

Table 1. Collision material properties.

Material Model	Size mm (Length, Width, Thickness)	Density ($g \cdot cm^{-3}$)	Young's Modulus (MPa)	Poisson's Ratio
Q235 Steel	140 × 75 × 7	7.85	2.10 × 105	0.25
Rubber	140 × 75 × 7	1.8	100	0.30

2.2. Experimental Setup

To measure the collision recovery coefficient between wheat grain and collision material, a kinematic model of the grain impact process was established, and a test apparatus for grain elasticity recovery coefficient was constructed as illustrated in Figure 1. The test apparatus primarily consists of the overall support of the test bench, the grain collection plane, the collision plate or the loss sensor striking the force plate, the grain feeding mechanism, and the grain height lifting lead screw. The collision plate was mounted at a 45-degree angle in front of the grain collection plane of the test bench, and the wheat grain sample was positioned in the grain dispensing mechanism directly above.

2.3. Test Principle

Collision represents a prevalent mechanical phenomenon, characterized by a brief duration of the collision process [12], minimal displacement of the colliding objects, considerable velocity alterations, substantial impact force exerted by the colliding entities, and energy dissipation. Consider two objects possessing masses m_1 and m_2, colliding at velocities v_1 and v_2, respectively. In accordance with the conservation of momentum principle, the momentum conversion formula during the collision process involving these two objects can be deduced, as demonstrated in Equation (1) [13]:

$$\begin{cases} m_1 v_1 + m_2 v_2 = m_1 v_1' + m_2 v_2' \\ k = \frac{v_2' - v_1'}{v_1 - v_2} \end{cases} \quad (1)$$

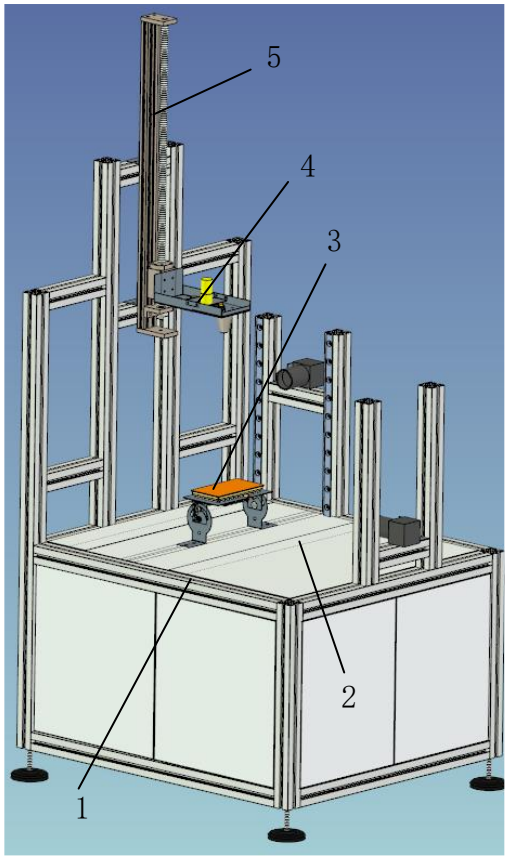

Figure 1. Grain impact test bench. 1. test bed bracket; 2. grain collection plane; 3. collision plate; 4. grain delivery mechanism; 5. grain height lifting screw.

After derivation and calculation, velocities v_1 and v_2 after the collision can be ascertained, as indicated in Equation (2):

$$\begin{cases} v_1' = v_1 - (1+k)\frac{m_2}{m_1+m_2}(v_1 - v_2) \\ v_2' = v_2 + (1+k)\frac{m_1}{m_1+m_2}(v_1 - v_2) \end{cases} \tag{2}$$

when k is equal to 1,

$$\begin{cases} v_1' = v_1 - \frac{2m_2}{m_1+m_2}(v_1 - v_2) \\ v_2' = v_2 + \frac{2m_1}{m_1+m_2}(v_1 - v_2) \end{cases} \tag{3}$$

when k is equal to 0,

$$v_1' = v_2' = \frac{m_1 v_1 + m_2 v_2}{m_1 + m_2} \tag{4}$$

where m_1 and m_2 denote the masses of the two colliding objects, with the unit in kg. v_1 and v_2 represent the pre-collision velocities of the two colliding objects, expressed in m/s; and v_1 and v_2 correspond to the post-collision velocities of the objects, with the unit in m/s. The reference formatting has been adjusted.

Upon analyzing Equations (3) and (4), it becomes apparent that the k value dictates the post-collision velocity alteration of the objects. When k = 1, a perfect elastic collision transpires, and the velocities of the two objects are transferred. Notably, when m_1 = m_2, the velocities of the two objects are exchanged following the collision. When k = 0, an imperfectly elastic collision occurs. Post-collision, the velocities become identical and the two objects proceed in unison.

In addition to their velocity, the kinetic energy of the two objects undergoes alteration following the collision, with the most pronounced change being kinetic energy loss.

Equation (5) illustrates the pre- and post-collision kinetic energy equation, with T_1 and T_2 representing the cumulative kinetic energy before and after the collision, respectively.

$$\begin{cases} T_1 = \frac{1}{2}m_1v_1^2 + \frac{1}{2}m_2v_2^2 \\ T_2 = \frac{1}{2}m_1v_1'^2 + \frac{1}{2}m_2v_2'^2 \end{cases} \tag{5}$$

The total kinetic energy loss of the two objects post-collision can be derived, as displayed in Equation (6):

$$\begin{aligned} \triangle T &= T_1 - T_2 \\ &= \frac{m_1m_2}{2(m_1+m_2)}(1+k)^2(v_1-v_2)^2 \end{aligned} \tag{6}$$

when k = 1, kinetic energy loss is expressed as Equation (7):

$$\triangle T = T_1 - T_2 = 0 \tag{7}$$

where T_1 signifies the aggregate kinetic energy of the two objects prior to the collision, with the unit in J; T_2 represents the total kinetic energy of the two bodies following the collision, with the unit in J; and ΔT denotes the difference in kinetic energy between the two objects pre- and post-collision, expressed in J.

When k = 0, kinetic energy loss is expressed as Equation (8):

$$\triangle T = \frac{m_1m_2}{2(m_1+m_2)}(v_1-v_2)^2 \tag{8}$$

In accordance with the definition of the recovery coefficient e (both e and k are designated as elastic recovery coefficients), the proportion of the separation velocities of two objects in the normal direction at the contact point before and after collision represents the elastic recovery coefficient. Consequently, a schematic illustration of the determination of the elastic recovery coefficient is depicted in Figure 2. It is merely necessary to obtain the approaching velocity prior to the collision and the separating velocity following the collision to deduce the elastic recovery coefficient. To enhance the precision of velocity detection, this test employs the principle of kinematic equations, calculating the requisite velocity values through an indirect method.

After the grain experiences impact and rebound, a parabolic trajectory is formed, where s signifies the horizontal displacement following the grain rebound, and h represents the distance from the grain collection plane to the rebound point. From this, the x-axis directional velocity after the collision can be determined, as demonstrated in Equation (9):

$$v_x = s\sqrt{\frac{g}{2h}} \tag{9}$$

where s denotes the horizontal displacement of seeds post-rebound, with the unit being millimeters; h is the vertical distance between the rebound point and the grain collection plane (unit: mm). Additionally, g corresponds to neutral acceleration, measured in m/s^2; v_x refers to the velocity along the x-axis after the grain collision, with the unit expressed in m/s.

The grain descends from the feeding mechanism, undergoing free-fall motion, with H being the distance from the seed falling point to the impact point. From this information, the y-axis directional velocity prior to grain collision can be calculated, as shown in Equation (10):

$$v_y = \sqrt{2gH} \tag{10}$$

where H is the height of grain fall and the unit is mm.

Finally, the formula for computing the recovery coefficient is derived by utilizing the definition of the recovery coefficient, as presented in Equation (11). In this equation, θ symbolizes the angle between the Y-axis velocity and the normal vector velocity before

grain collision, while β represents the angle between the X-axis direction velocity and the normal vector velocity prior to grain collision.

$$e = \frac{v_1}{v_0} = \frac{v_x \cos\beta}{v_y \cos\theta} = \frac{s\cos\beta}{2\cos\theta\sqrt{Hg}} \tag{11}$$

where e refers to the elastic recovery coefficient, θ is the angle between the velocity along the Y-axis and the normal vector preceding grain collision, and β is the angle between the velocity along the X-axis and the normal vector before the grain collision.

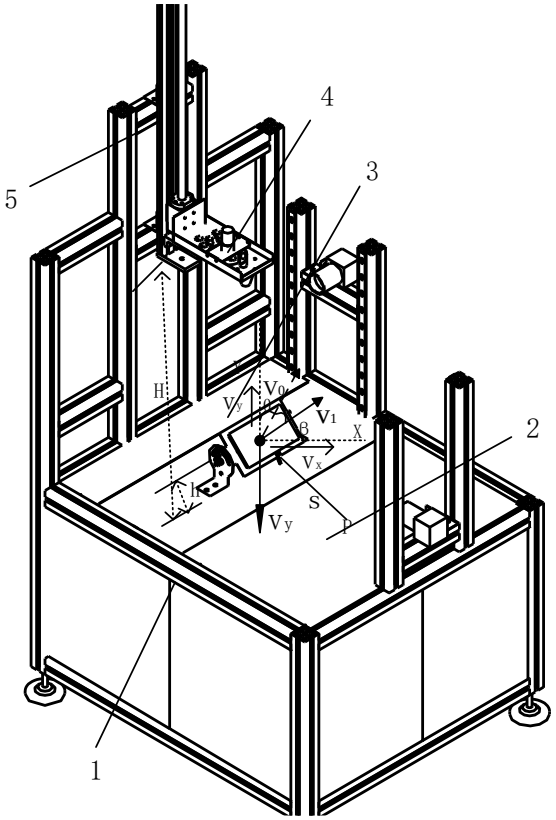

Figure 2. Schematic diagram of elastic recovery coefficient determination. 1. test bed bracket; 2. grain collection plane; 3. collision plate; 4. grain delivery mechanism; 5. grain height lifting screw.

2.4. Experimental Methods

The wheat recovery coefficient primarily correlates with moisture content, collision material, material thickness, and fall height of wheat. To emulate the actual harvest scenario, wheat samples with varying moisture contents of 10%, 13%, 15%, and 18% were employed in the experiment. The chosen materials comprise Q235 steel plate and rubber; the material thicknesses selected are 2 mm, 4 mm, and 8 mm; the seed drop heights are 120 mm, 180 mm, and 240 mm; and the factor levels constituting the wheat univariate test are presented in Table 2.

Table 2. The level of univariate test factors.

Trial Level	Water Content (%)	Collision Materials	Material Thickness (mm)	Drop Height (mm)
1	10	Q235 Steel	2	120
2	13	Rubber	4	180
3	15	/	8	240
4	18	/	/	/

/: indicates that no data exists.

In accordance with the factor level in Table 2, four sets of single-factor influence tests were conducted. In the test on the effect of moisture content on the recovery coefficient, Q235 steel served as the collision material, the material thickness remained at 4 mm, and the drop height was set at 180 mm, resulting in four sets of data. In the test regarding the impact of collision material on the wheat recovery coefficient, the material thickness remained at 4 mm, and the drop height was set at 180 mm, yielding eight sets of data. In the test regarding the effect of material thickness on the wheat recovery coefficient, Q235 steel served as the collision material, and the drop height was set at 180 mm, procuring 12 sets of data under distinct moisture conditions. In the test regarding the impact of fall height on the wheat recovery coefficient, Q235 steel served as the collision material, and the material thickness remained at 4 mm, obtaining 12 sets of data under varying moisture conditions.

3. Results and Analysis

3.1. Effect of Moisture Content on Recovery Coefficient of Wheat

The experimental data corresponding to various moisture content levels are presented in Table 3. From this information, a trend figure (Figure 3) illustrating the factors influencing single-factor water content on the recovery coefficient can be derived. The analysis reveals that under the test premise of employing Q235 steel as the collision material, maintaining material thickness at 4 mm, and setting the drop height at 180 mm, the recovery coefficient of wheat is significantly impacted by moisture content. As moisture content increases, the recovery coefficient progressively declines.

Table 3. Moisture content univariate experimental data.

NO	Whereabouts Height (mm)	Material Thickness (mm)	Collision Materials	Water Content (%)	Recovery Factor
1	180	4	Q235 Steel	10	0.4826
2	180	4	Q235 Steel	13	0.4651
3	180	4	Q235 Steel	15	0.4598
4	180	4	Q235 Steel	18	0.4276

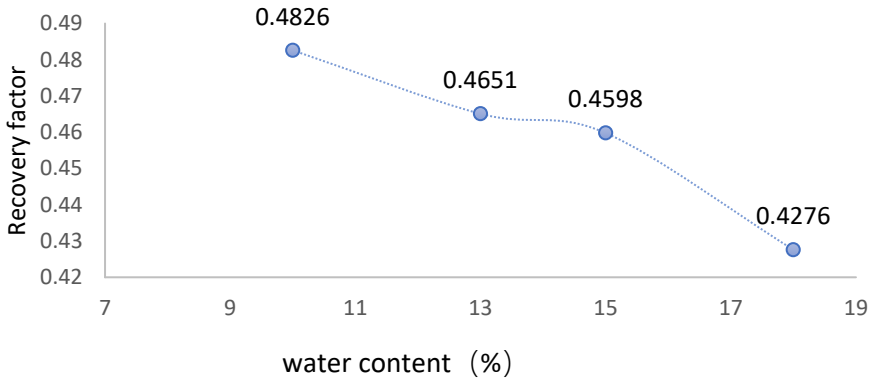

Figure 3. Trend of recovery coefficient of factors influencing single-factor moisture content.

3.2. Influence of Collision Materials on Wheat Recovery Coefficient

Table 4 displays experimental data related to different collision materials. A bar chart depicting the recovery coefficient of single-factor collision material can be generated (Figure 4). Analysis indicates that when material thickness remains fixed at 4 mm and the drop height is set at 180 mm for the test, the recovery coefficient of wheat is notably affected by the collision material. The recovery coefficient for grain collision involving rubber material across four moisture levels is lower than that of Q235 steel, which can be attributed to the soft texture of the rubber and the partial absorption of collision energy.

Table 4. Single-factor experimental data of collision materials.

NO	Whereabouts Height (mm)	Material Thickness (mm)	Water Content (%)	Collision Materials	Recovery Factor
1	180	4	10	Q235 Steel	0.4826
2	180	4	13	Q235 Steel	0.4651
3	180	4	15	Q235 Steel	0.4598
4	180	4	18	Q235 Steel	0.4276
5	180	4	10	Rubber	0.4716
6	180	4	13	Rubber	0.4521
7	180	4	15	Rubber	0.4306
8	180	4	18	Rubber	0.4086

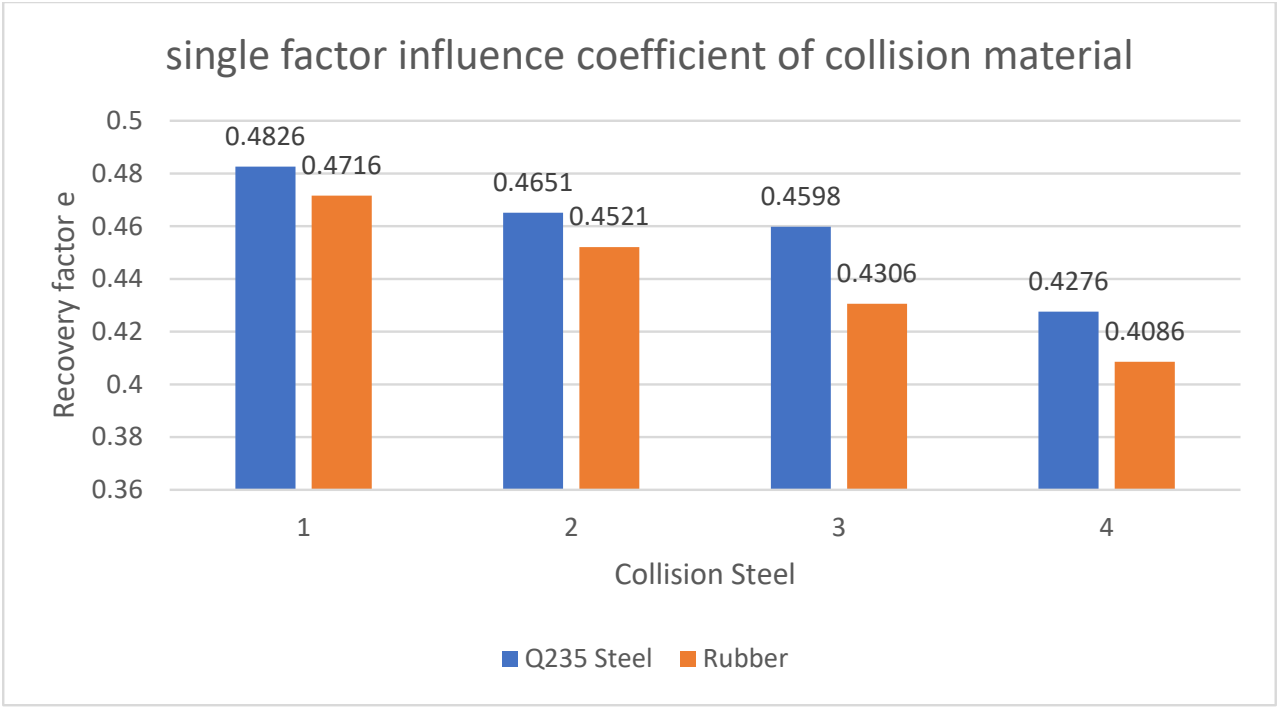

Figure 4. Single factor of collision material affects recovery factor.

3.3. Effect of Material Thickness on Wheat Recovery Coefficient

Table 5 presents experimental data for different material thicknesses. A distribution map of the factors influencing single-factor material thickness on the recovery coefficient can be created (Figure 5). Analysis demonstrates that under the test premise of utilizing Q235 steel for the collision material and maintaining the drop height at 180 mm, the recovery coefficient of wheat exhibits an increasing trend as material thickness grows. When the thickness reaches approximately 7 mm, the increase in recovery coefficient levels off and stabilizes. Material thickness directly reflects the stiffness properties of the material. As material thickness increases, stiffness follows suit. Consequently, when wheat deformation is reduced during collision events, energy loss also decreases, resulting in a larger elastic recovery coefficient.

Table 5. Material thickness unifactor experimental data.

NO	Whereabouts Height (mm)	Collision Materials	Material Thickness (mm)	Water Content (%)	Recovery Factor
1	180	Q235 Steel	2	10	0.4712
2	180	Q235 Steel	2	13	0.4535
3	180	Q235 Steel	2	15	0.4376
4	180	Q235 Steel	2	18	0.4109
5	180	Q235 Steel	4	10	0.4826
6	180	Q235 Steel	4	13	0.4651
7	180	Q235 Steel	4	15	0.4598
8	180	Q235 Steel	4	18	0.4276
9	180	Q235 Steel	8	10	0.4915
10	180	Q235 Steel	8	13	0.4721
11	180	Q235 Steel	8	15	0.4644
12	180	Q235 Steel	8	18	0.4309

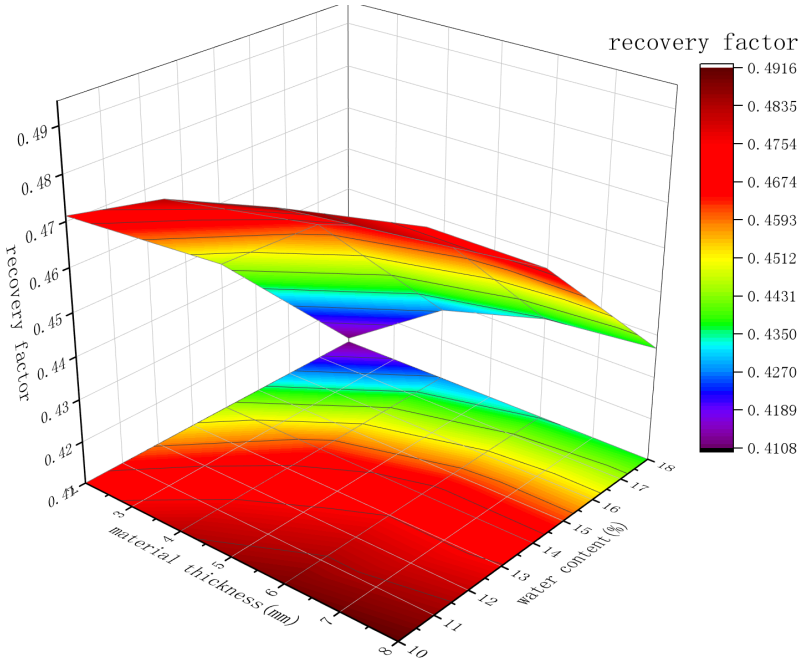

Figure 5. Single factor of material thickness affects the recovery factor.

3.4. Effect of Drop Height on Wheat Recovery Coefficient

The data from experiments with varying fall heights are presented in Table 6, from which a univariate fall height influence factor recovery coefficient distribution map can be derived, as depicted in Figure 6. Upon analysis, it becomes evident that, when utilizing Q235 steel as the collision material and maintaining a constant material thickness of 4 mm, the falling height of wheat grains exerts an influence on the recovery coefficient. For wheat with different moisture content, the impact of falling height on the recovery coefficient remains relatively consistent. As the fall height of wheat grains increases, the recovery coefficient between them and the collision material diminishes. This phenomenon can be attributed to the rising falling height of wheat particles, which leads to increased deformation during collisions with the test plate and heightened frictional resistance between the air and the collision plate. Consequently, the energy loss of wheat particles escalates during the collision process, causing the rebound velocity of grains to decrease after the collision and subsequently leading to a reduced recovery coefficient, as calculated based on the principle of elastic recovery coefficient.

Table 6. Single-factor experimental data of drop height.

NO	Collision Materials	Material Thickness (mm)	Drop Height (mm)	Water Content (%)	Recovery Factor
1	Q235 Steel	4	120	10	0.4968
2	Q235 Steel	4	180	13	0.4651
3	Q235 Steel	4	240	15	0.4368
4	Q235 Steel	4	120	18	0.4384
5	Q235 Steel	4	180	10	0.4826
6	Q235 Steel	4	240	13	0.4501
7	Q235 Steel	4	120	15	0.4735
8	Q235 Steel	4	180	18	0.4276
9	Q235 Steel	4	240	10	0.4685
10	Q235 Steel	4	120	13	0.4763
11	Q235 Steel	4	180	15	0.4598
12	Q235 Steel	4	240	18	0.4167

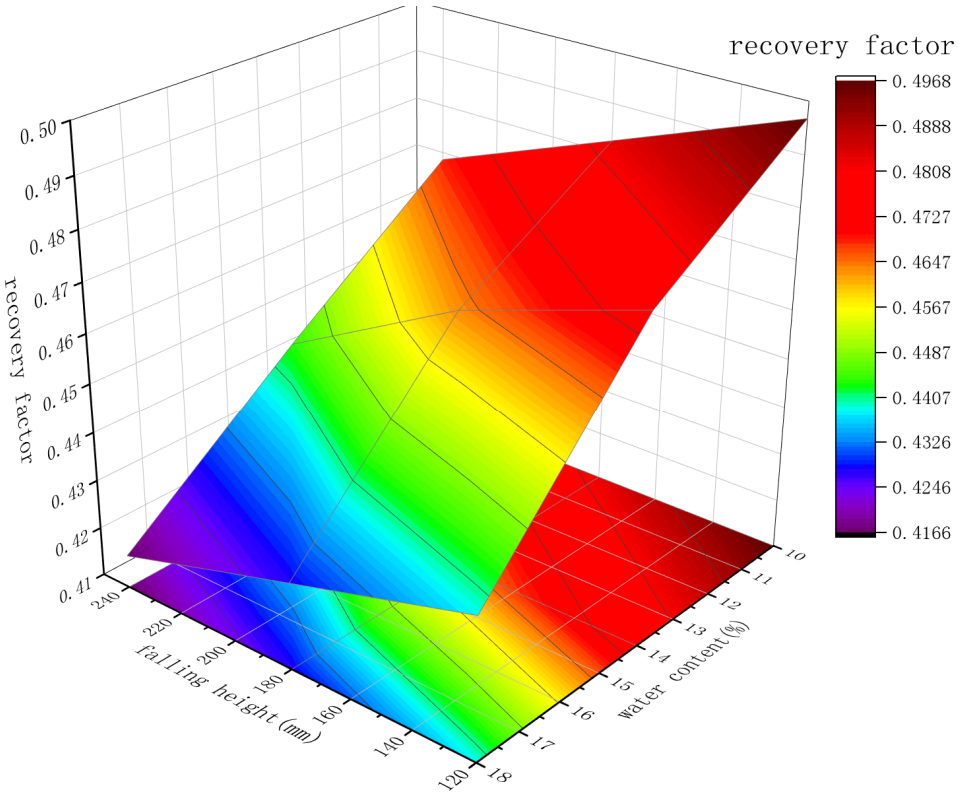

Figure 6. Single factor of fall height affects the recovery coefficient.

4. Conclusions

(1) The collision material influences the deformation and recovery capacity of wheat during collisions, serving as the primary factor affecting the recovery coefficient in wheat collision experiments. Given constant drop height, material thickness, and moisture content, the elastic recovery coefficient of wheat and rubber in this test is lower than that of wheat and Q235 steel. Therefore, during the mechanical design process for wheat, material selection should be tailored to the specific context.

(2) The falling height dictates the energy changes as the wheat grain collides with the test board material, particularly affecting the size of the wheat shape variable and the movement resistance. When the falling height increases, the grain shape variable expands, and the movement resistance rises correspondingly, leading to a reduced elastic recovery coefficient. The stiffness of the material is determined by its thickness, with an increase in material thickness enhancing the stiffness. When wheat grains come into contact with the

collision material, their energy loss decreases, the initial rebound velocity grows, and, in turn, the elastic recovery coefficient is elevated.

(3) Wheat grains interact with different materials during the collision process, undergoing force deformation and rebound recovery in two separate movement phases. Following the collision, wheat grains may also exhibit rotation and other factors. Consequently, the recovery coefficient of wheat for the same material with varying parameters in the collision material yields a wide range of recovery coefficient changes. The test process revealed that the same wheat grain produced varying test results in multiple tests.

Author Contributions: Conceptualization, J.W. and F.W.; methodology, Y.L.; software, W.Z.; validation, B.Z., X.F. and J.W.; formal analysis, W.Z.; investigation, Y.L.; resources, B.Z.; data curation, J.W.; writing—original draft preparation, J.W.; writing—review and editing, F.W.; visualization, Y.L.; supervision, W.Z.; project administration, J.W.; funding acquisition, W.Z. All authors have read and agreed to the published version of the manuscript.

Funding: This research was funded by the National Key Research and Development Program Project of China (2021YFD2000601).

Informed Consent Statement: Not applicable.

Data Availability Statement: Not applicable.

Conflicts of Interest: The authors declare no conflict of interest.

References

1. Ning, X.J.; Jin, C.Q.; Li, Q.L. Determination and analysis of physical characteristics of two soybean extractables in Huang-Huai-Hai area. *J. Agric. Mech. Res.* **2021**, *43*, 163–168, 175.
2. Liu, F.Y.; Zhang, J.; Li, B. Discrete element parameter analysis and calibration of wheat based on packing test. *Trans. Chin. Soc. Agric. Eng.* **2016**, *32*, 247–253.
3. Li, X.F.; Liu, F.; Zhao, M.Q. Determination of contact parameters between maize seeds and seeders. *J. Agric. Mech. Res.* **2018**, *40*, 149–153.
4. Kong, F.T.; Shi, L.; Zhang, Y.T. Determination and analysis of recovery coefficient in seed cotton collision model. *China Agric. Sci. Technol. Rev.* **2019**, *21*, 92–99. [CrossRef]
5. Liu, Y.; Zong, W.Y.; Ma, L.N. Determination of 3D collision recovery coefficient of oil sunflower seeds by high-speed photography. *Trans. Chin. Soc. Agric. Eng.* **2020**, *36*, 44–53.
6. Wen, E.Y.; Li, Y.H.; Niu, Z. Garlic seed particle discrete element model parameter calibration. *Agric. Mech. Res.* **2021**, *43*, 160–167. [CrossRef]
7. Zhang, Y.; Liu, F.; Zhao, M.Q. Experimental study on Physical and mechanical characteristics of Mung bean. *J. Agric. Mech. Res.* **2017**, *39*, 119–124.
8. Patil, D.; Higgs, C.F. Experimental investigations on the coefficient of restitution for Sphere-Thin plate elastoplatic impact. *J. Tribol.* **2018**, *140*, 011406. [CrossRef]
9. Chen, D.Y.; Yang, Z.; La, G.X. Determination of collision recovery coefficient in half-summer harvest. *Agric. Eng.* **2021**, *11*, 82–88. [CrossRef]
10. Zheng, H.B. *Simulation and Experimental Verification of Pyrolysis Motion-Heat Transfer Coupling Relationship in Waste Tire Rotary Kiln*; Southeast University: Nanjing, China, 2021.
11. Zheng, J. *Design and Test of American Ginseng Pneumatic Needle Precision Collector*; Huazhong Agricultural University: Wuhan, China, 2019.
12. Rezaiee-Pajand, M.; Mokhtari, M.; Masoodi, A.R. Stability and free vibration analysis of tapered sandwich columns with functionally graded core and flexible connections. *CEAS Aeronaut. J.* **2018**, *9*, 629–648. [CrossRef]
13. Li, Y.L.; Qiu, X.M.; Zhang, X. Analysis of different definitions of recovery coefficients and their applicability. *Mech. Pract.* **2015**, *37*, 773–777.

Disclaimer/Publisher's Note: The statements, opinions and data contained in all publications are solely those of the individual author(s) and contributor(s) and not of MDPI and/or the editor(s). MDPI and/or the editor(s) disclaim responsibility for any injury to people or property resulting from any ideas, methods, instructions or products referred to in the content.